LITHOS 440-441 (2023) 107030

Contents lists available at ScienceDirect

LITHOS

journal homepage: www.elsevier.com/locate/lithos

Boron isotope variations in a single monogenetic cone: La Poruña (21°53′S, 68°30′W), Central Andes, Chile

Benigno Godoy [a,*], Frances M. Deegan [b,*], Osvaldo González-Maurel [c], Petrus le Roux [c], Dieter Garbe-Schönberg [d,e], Inés Rodríguez [f,g], Gabriela Guzmán-Marusic [g], Carolina Marín [h]

[a] Centro de Excelencia en Geotermia de los Andes (CEGA), Departamento de Geología, Facultad de Ciencias Físicas y Matemáticas, Universidad de Chile, Plaza Ercilla 803, Santiago, Chile
[b] Department of Earth Sciences, Section for Natural Resources and Sustainable Development (NRHU), Uppsala University, 75236 Uppsala, Sweden
[c] Department of Geological Sciences, University of Cape Town, Rondebosch 7700, South Africa
[d] Institute of Geosciences, Kiel University, 24118 Kiel, Germany
[e] Department of Physics and Earth Sciences, Jacobs University Bremen, 28759 Bremen, Germany
[f] Departamento de Obras Civiles y Geología, Facultad de Ingeniería, Universidad Católica de Temuco, Rudecindo Ortega 02950, Temuco, Chile
[g] Centro de Investigación en Evaluación de Riesgos y Mitigación de Peligros Geológicos, Geokimün, Facultad de Ingeniería, Universidad Católica de Temuco, Rudecindo Ortega 02950, Temuco, Chile
[h] Teck Resources Chile Limitada, Alonso de Cordova 4580, piso 10, Las Condes, Santiago, Chile

A R T I C L E I N F O

Keywords:
Central Andes
La Poruña
Boron isotopes
Crustal assimilation

A B S T R A C T

La Poruña is a monogenetic volcano located within the Altiplano-Puna Volcanic Complex (21°-24°S) in the Central Andean subduction zone. Since crustal contamination of Andean magmas is ubiquitous, and because extensive geochemical data exist for La Poruña, we employ this volcano as a case study to examine the behavior of boron isotopes during crustal assimilation. We present whole-rock boron concentration and $^{11}B/^{10}B$ ratios (as $\delta^{11}B$ values) for La Poruña lava samples that were prepared as nano-particulate pressed pellets. La Poruña B contents range from 14 to 20 μg/g and $\delta^{11}B$ values range from −1.39 ± 0.54 ‰ (2σ) to +0.94 ± 0.30 ‰ (2σ), which overlap with the range of available whole-rock data for Central Andean lavas. Moreover, La Poruña $\delta^{11}B$ values correlate negatively with $^{87}Sr/^{86}Sr$ ratios from the same samples. Since $^{87}Sr/^{86}Sr$ is a proxy for crustal contamination at La Poruña, the data lead us to suggest that La Poruña magmas assimilated a low-$\delta^{11}B$, high $^{87}Sr/^{86}Sr$ component such as Andean continental crust. Mixing models based on B and Sr isotopes support a broadly two-step magma evolution for La Poruña. In step 1, mantle-derived primary melts interacted with boron-rich slab-derived fluids with high $\delta^{11}B$ values, which yielded subduction-modified parental magmas with ca. 3 μg/g B and relatively high $\delta^{11}B$ values. In step 2, the high $\delta^{11}B$ parental magmas ascended through the crust where they assimilated up to 20% crustal material, which further modified their $\delta^{11}B$ values and $^{87}Sr/^{86}Sr$ ratios. In comparison to available regional values for B and $\delta^{11}B$, it appears that La Poruña and nearby volcanic centers shared a similar source and magmatic history, whereas volcanoes south of 23°S differ. We stress, however, that deconvolving the roles of various subduction and crustal inputs in the Central Andes would require further studies on individual volcanoes along the arc.

1. Introduction

Mantle hydration by slab-derived fluids plays a key role in the genesis of magmas in subduction-related tectonic environments. This process is driven by dehydration of hydrous minerals in the down-going slab, which triggers partial melting of the overlying mantle wedge (e.g. Ryan and Chauvel, 2014; Spandler and Pirard, 2013). Most igneous rocks in subduction zones have greater concentrations of boron than depleted mantle (MORB; Mid-Ocean Ridge Basalt) as well as low ratios of fluid-immobile elements to boron (e.g. Nb/B). These observations suggest that the greater boron contents of subduction zone lavas (also known as arc lavas) are due to boron transfer from slab-derived fluids to the mantle source region (e.g. Ishikawa and Tera, 1997; Rosner et al., 2003; Ryan and Chauvel, 2014). Boron isotope ratios [expressed as $\delta^{11}B$

* Corresponding authors.
E-mail addresses: bgodoy@uchile.cl (B. Godoy), frances.deegan@geo.uu.se (F.M. Deegan).

https://doi.org/10.1016/j.lithos.2023.107030
Received 9 June 2022; Received in revised form 9 January 2023; Accepted 13 January 2023
Available online 20 January 2023

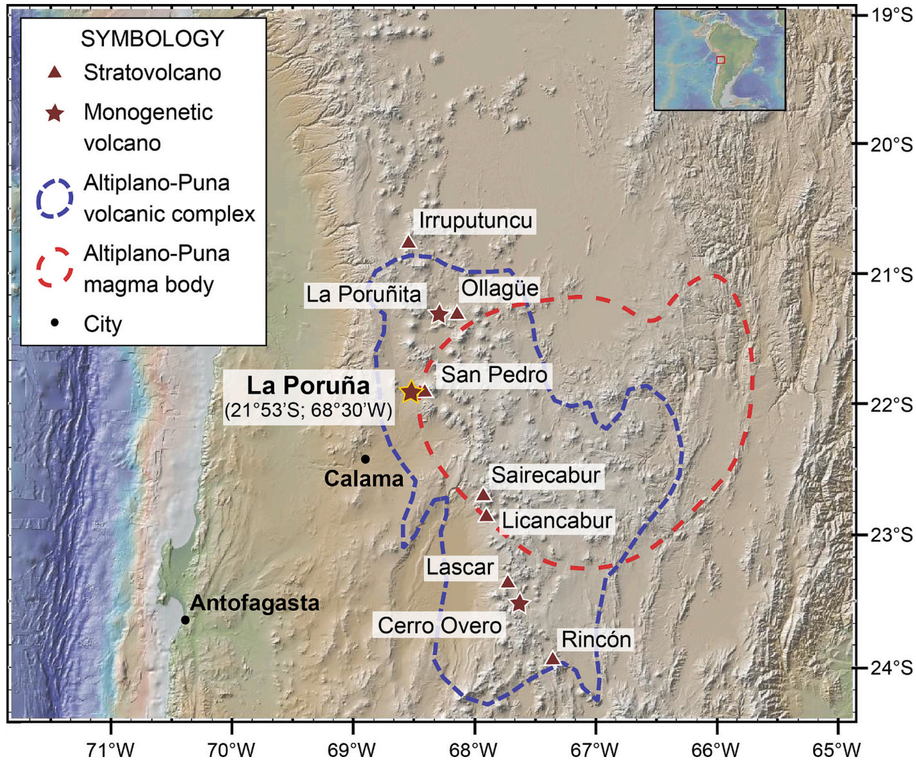

Fig. 1. Global Multi-Resolution Topography image showing the location of La Poruña and other volcanic structures within the Central Andes of northern Chile. The extent of the Altiplano-Puna Volcanic Complex (APVC; de Silva, 1989) and the surface projection of the Altiplano-Puna Magma Body (APMB; Ward et al., 2014) are indicated. Figure made with GeoMapApp (www.geomapapp.org; Ryan et al., 2009).

= (($^{11}B/^{10}B$(sample)/$^{11}B/^{10}B$(reference))-1) × 10^3 ‰] are useful tracers of various inputs to the subduction factory because during subduction and dehydration ^{11}B is preferentially fractionated into the fluid phase, which leads to the formation of boron enriched slab-derived fluids with high $\delta^{11}B$ values (e.g. Marschall et al., 2007; Peacock and Hervig, 1999; Ryan and Chauvel, 2014). Moreover, the $\delta^{11}B$ values of slab-derived fluids progressively evolve towards lower $\delta^{11}B$ values due to dehydration reactions and boron loss during subduction (e.g. Hervig et al., 2002; Konrad-Schmolke and Halama, 2014; Marschall et al., 2007; Peacock and Hervig, 1999). Therefore, fluids with variable $\delta^{11}B$ values can be produced during subduction and react with the mantle wedge to generate the large range of $\delta^{11}B$ values seen in global arc databases (see Deegan et al., 2016 for a summary). Once magma leaves its source and migrates to the surface it may interact with rocks comprising the upper arc crust. While the upper crust has a wide range of boron isotopic compositions, the $\delta^{11}B$ values of continental crust are often lower than arc magmas (e.g. Kasemann et al., 2000; Palmer and Swihart, 1996). Hence, boron isotopes have the potential to distinguish between different subduction-related processes such as source hydration, slab contribution, and crustal assimilation at active continental margins (e.g. de Hoog and Savov, 2018; Deegan et al., 2016; Gméling et al., 2007; Palmer, 2017; Rosner et al., 2003; Schmitt et al., 2002; Tonarini et al., 2001a, 2001b).

The Central Andes (14°-27°S) is a tectono-magmatic province formed due to subduction of the Nazca Plate below the South American Plate. The recent (<10 Ma) volcanic arc of the Central Andes was constructed mainly by eruption of andesitic-to-dacitic lavas and dacitic-to-rhyolitic ignimbrites (e.g. de Silva and Kay, 2018; Mamani et al., 2010; Trumbull et al., 2006; Wörner et al., 2018). Partial melting of the mantle wedge, driven by fluids released from the slab, is considered to be the primary process involved in generating magmas in the Central Andes (e.g. de Silva and Kay, 2018; Godoy et al., 2014; Matteini et al., 2002; Wörner et al., 2018). After magma leaves its source region, magmatic differentiation involves significant degrees of crustal assimilation due the exceptional thickness of the continental crust below the volcanic arc, as reflected by radiogenic and stable isotopes signatures of erupted lavas (e.g. Godoy et al., 2014, 2017; González-Maurel et al., 2019a, 2020; Matteini et al., 2002; Michelfelder et al., 2013; Rosner et al., 2003; van Alderwerelt et al., 2021; Wörner et al., 2018).

To date, boron isotope studies of Central Andean rocks, minerals, and melt inclusions have mainly focused on characterizing specific geochemical reservoirs (e.g. upper continental crust; Kasemann et al., 2000) and investigating large-scale regional and temporal variations along the arc (Jones et al., 2014; Rosner et al., 2003). However, detailed boron isotope studies constraining the evolution of single volcanic systems are lacking. The purpose of this work, therefore, is to focus on boron isotope variations at the scale of a single monogenetic volcano where there exist abundant contextual geochemical data. To accomplish this, we selected La Poruña volcano (21°53′S, 68°30′W; Fig. 1), which is a young (<100 ka; Wörner et al., 2000; González-Maurel et al., 2019b) volcanic system in the Central Andes that is notable for its eruption of mafic lavas that record isotopic evidence for crustal assimilation (González-Maurel et al., 2019a, 2020). Here we present new boron elemental and isotopic data for five whole-rock lava samples from La Poruña and compare them to available data for other volcanoes in the Central Andes (Fig. 1). Although our sample set is relatively small, the samples are geochemically well characterized, which makes La Poruña a good natural laboratory to study the behavior of boron isotopes during magmatic evolution in the Central Andes.

2. Geological background

The current volcanic front of the Central Andes is a subduction-related arc in which primary magmatism is associated with partial melting triggered by hydration of the mantle wedge by slab fluids (e.g. Godoy et al., 2014; Matteini et al., 2002; Wörner et al., 2018). This volcanic arc is constructed on thick continental crust (>60 km; Beck et al., 1996; Prezzi et al., 2009) on which the recent (<10 Ma) volcanism

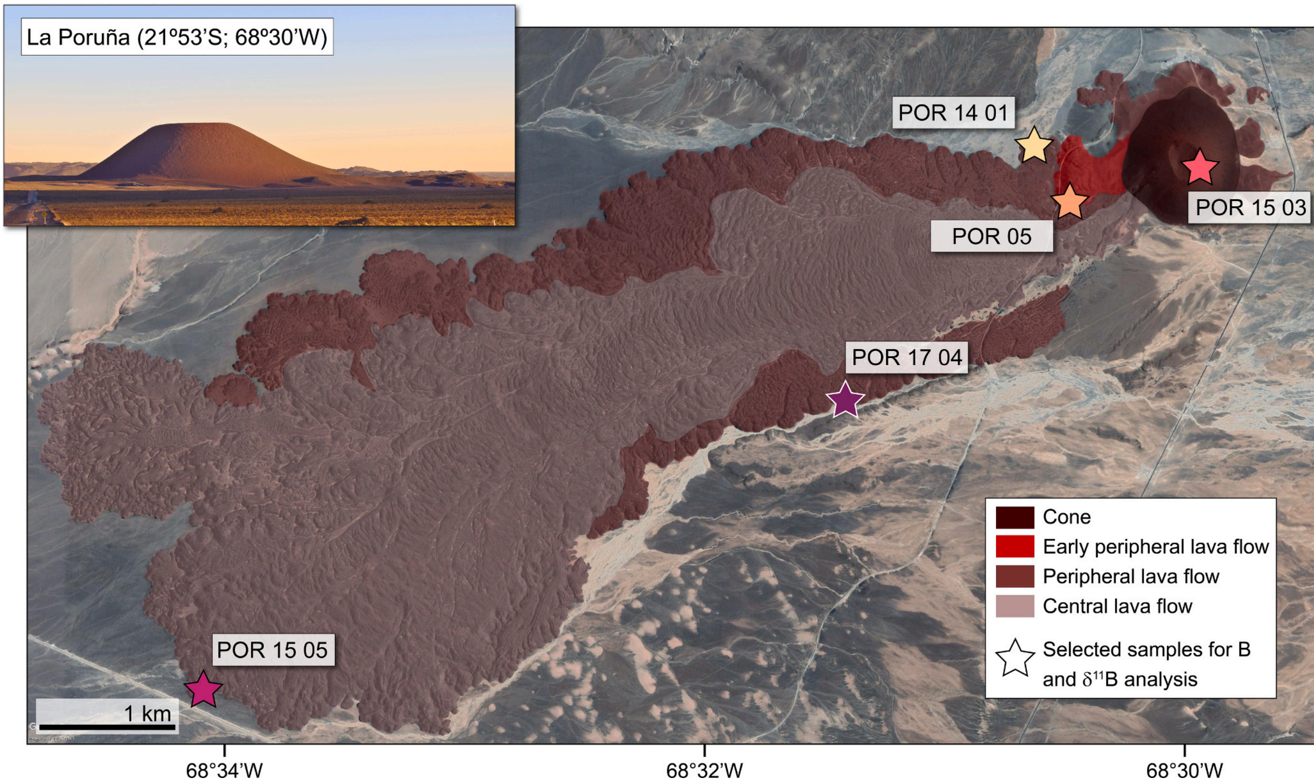

Fig. 2. Satellite image (Google Earth™) showing the different lithofacies of La Poruña (after Marín et al., 2020). Locations of samples selected for boron isotope analysis in this study are also shown (samples are color-coded to Fig. 3).

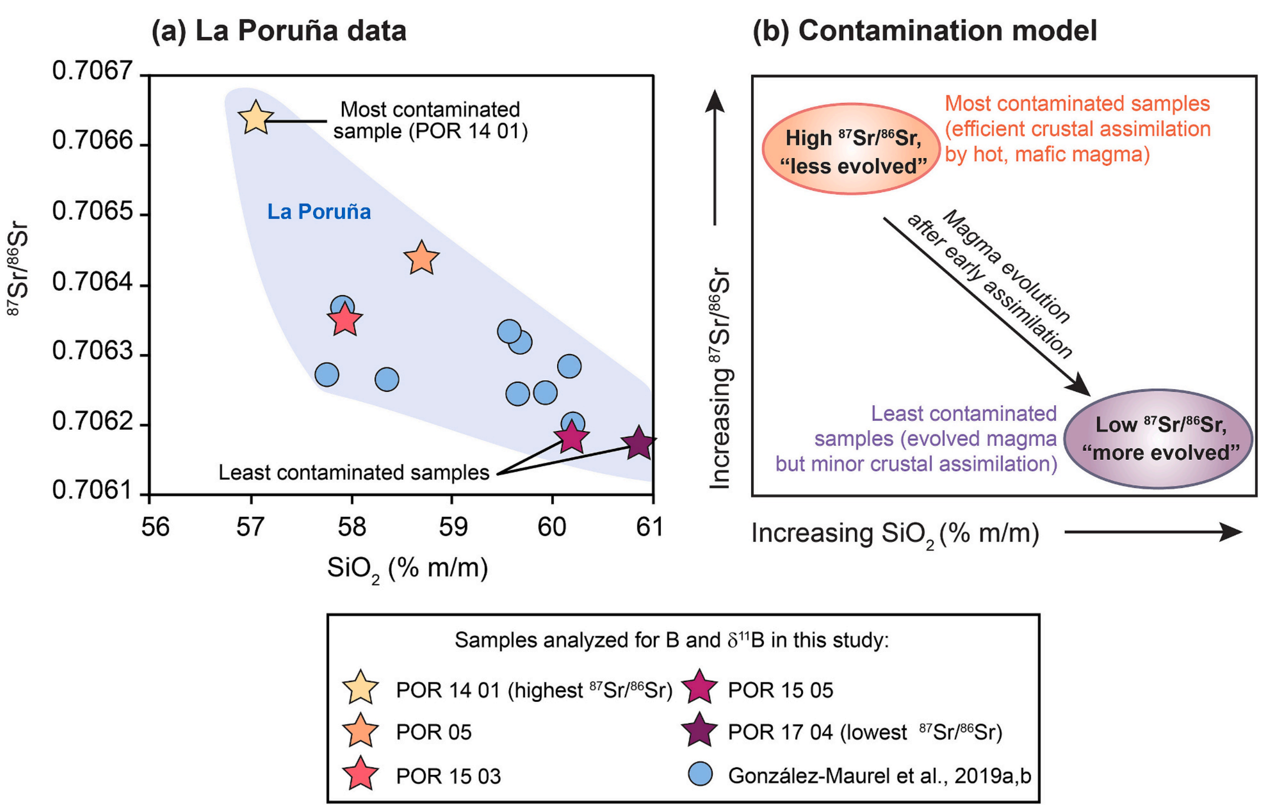

Fig. 3. $^{87}Sr/^{86}Sr$ vs SiO_2 (% m/m) diagram showing (a) the composition of samples from La Poruña (data from González-Maurel et al., 2019a, 2019b), and (b) the proposed crustal contamination model. Note that at La Poruña, $^{87}Sr/^{86}Sr$ is used as a proxy for crustal contamination, where relatively high $^{87}Sr/^{86}Sr$ ratios in lava samples indicate that the corresponding magma assimilated continental crust with high $^{87}Sr/^{86}Sr$ ratios. Stars indicate the samples selected for boron isotope analysis in this study (for sample locations see Fig. 2). Error bars are smaller than symbol size.

Table 1
Geochemical characteristics of the analyzed samples.

Sample	Latitude	Longitude	SiO_2[*,a]	Nb (μg/g)[a]	$^{87}Sr/^{86}Sr$[a]	2σ (10^{-6})[a]	B (μg/g)	$\delta^{11}B$ (‰)	2σ (‰)[b]	$\delta^{11}B$ (‰)	2σ (‰)	$\delta^{11}B$ (‰)	2σ (‰)	$\delta^{11}B$ (‰)	2σ (‰)	$\delta^{11}B$ (‰)	2σ (‰)
								Sample mean		*$\delta^{11}B$ values of individual spot analyses*							
POR 14 01	21° 53′ 27″	68° 30′ 39″	57.05	6.71	0.706640	8.10	17	−1.39	0.54	−0.77	0.21	−1.35	0.15	−1.53	0.17	−1.91	0.17
POR 15 03	21° 53′ 32″	68° 29′ 58″	57.93	6.09	0.706353	12.6	14	−0.14	0.30	+0.03	0.24	−0.02	0.23	−0.35	0.13	−0.23	0.10
POR 15 05	21° 55′ 32″	68° 34′ 2″	60.18	6.23	0.706184	9.62	17	+0.38	0.43	0.70	0.17	+0.23	0.17	+0.21	0.18	–	–
POR 17 04	21° 54′ 55″	68° 32′ 25″	60.86	6.20	0.706176	11.0	20	+0.94	0.30	+1.03	0.15	+0.67	0.11	+1.02	0.14	+1.06	0.12
POR-05	21° 53′ 42″	68° 30′ 31″	58.70	6.55	0.706441	10.0	14	−0.12	0.34	+0.21	0.22	−0.12	0.21	−0.26	0.21	−0.30	0.16
Reference materials analyzed as unknowns																	
JR-1	This study						130	+3.01	0.26	+2.85	0.05	+3.06	0.07	+3.07	0.08	+3.05	0.08
	Gangjian et al., 2013							+2.80	0.20								
JR-2	This study						140	+2.70	0.32	+2.55	0.08	+2.78	0.07	+2.77	0.06	–	–
	Gangjian et al., 2013							+2.70	0.20								
JB-3	This study						20	+6.02	0.26	+5.93	0.16	+5.99	0.11	+6.02	0.16	+6.15	0.18
	Gangjian et al., 2013							+5.60	0.10								
JA-2	This study						20	−9.65	0.26	−9.54	0.12	−9.63	0.17	−9.71	0.16	−9.73	0.11
	Gangjian et al., 2013							−9.30	0.40								
Additional reference materials																	
JB-2	Liu et al., 2018						27	+7.12	0.2								

[*] SiO_2 recalculated to 100% (m/m) water free.
[a] Data after González-Maurel et al., 2019a, 2019b.
[b] Full error propagation considering measurements of the samples and reference material (JB-2), error on the value used for the reference material, and error on the value used for NIST951 ($^{11}B/^{10}B = 4.04362 \pm 0.001$ 2σ; Liu et al., 2018).

developed (e.g. Godoy et al., 2017; Mamani et al., 2010; Trumbull et al., 2006; Wörner et al., 2018). The Altiplano-Puna Volcanic Complex (21°-24°S, de Silva, 1989) (Fig. 1) is a tectono-magmatic province within the Central Andes where an upper crustal (4–25 km below the surface) partially molten layer, the Altiplano-Puna Magma Body (Fig. 1), has been geophysically constrained (e.g. Chmielowski et al., 1999; Spang et al., 2021; Ward et al., 2014; Zandt et al., 2003). It has previously been suggested that the petrogenesis of erupted lavas of the Altiplano-Puna Volcanic Complex involved variable degrees of contamination by partial melts of the Altiplano-Puna Magma Body as well as the thick Andean continental crust (e.g. Feeley and Davidson, 1994; Godoy et al., 2017; González-Maurel et al., 2019a, 2020; Michelfelder et al., 2013; Rosner et al., 2003; van Alderwerelt et al., 2021; Wörner et al., 2018).

La Poruña (21°53′S, 68°30′W) is a monogenetic volcanic structure located in the volcanic front of the Altiplano-Puna Volcanic Complex (Fig. 1). La Poruña consists of a scoria cone from which at least two lava flows erupted at ca. 100 ka (González-Maurel et al., 2019b; Marín et al., 2020) (Fig. 2). A detailed description of the lithofacies associated with the cone and the lava flows of La Poruña suggests different eruptive styles, which varied from Strombolian to effusive (Marín et al., 2020). Petrographic characteristics of samples from the scoria cone and the lava flows are similar (based on point counting and automated SEM mineralogical analysis; González-Maurel et al., 2019b and Marín et al., 2020). The main mineralogical assemblage at La Poruña includes plagioclase + orthopyroxene + clinopyroxene ± olivine ± amphibole phenocrysts (>0.5 mm) at ca. 5–40 vol% set in a groundmass of ca. 30–50 vol% consisting of glass and minor amounts of plagioclase + orthopyroxene + clinopyroxene ± olivine (González-Maurel et al., 2019b; Marín et al., 2020). The vesicle content of the erupted products varies from <5 vol% (Lithofacies Lava Flow Central; Fig. 2) to ca. 40 vol% (Lithofacies Cone and Lava Flow Peripheral; Fig. 2) (González-Maurel et al., 2019b; Marín et al., 2020).

Volcanism at La Poruña was likely supplied by a relatively primitive sub-arc parental magma that underwent moderate degrees of crustal contamination (<28%) *en route* to the surface (Godoy et al., 2017; González-Maurel et al., 2020). The mechanism of magma-crust interaction at La Poruña has been suggested to have been via "assimilation during turbulent ascent" (Godoy et al., 2020; González-Maurel et al., 2019b). In this model, assimilation of crustal material was more significant in the presence of hot, mafic magma and the degree of crustal assimilation decreased with increasing magmatic differentiation due to the changing thermal conditions over time (cf. Huppert and Sparks, 1985). As a consequence, the less evolved samples record the highest degree of crustal assimilation, i.e. samples with relatively low SiO_2 have high $^{87}Sr/^{86}Sr$ ratios (see González-Maurel et al., 2019b; Godoy et al., 2020). The $^{87}Sr/^{86}Sr$ ratio of the La Poruña samples is therefore used as a proxy for crustal contamination in this paper, as outlined in Fig. 3.

3. Analytical methods

3.1. Sample selection

Five samples from La Poruña were selected for whole-rock boron elemental and isotopic analysis. All samples are fresh and show no obvious signs of alteration. One sample is from the cone (POR 15 03), one is from the central flow (POR 15 05), and three are from the peripheral flow (POR 05; POR 14 01; POR 17 04) (Fig. 2). The selected samples encompass the full range of $^{87}Sr/^{86}Sr$ ratios for La Poruña (Fig. 3). Detailed petrographic descriptions of the samples are provided by González-Maurel et al. (2019b) and Marín et al. (2020). Geochemical data including major and trace elements and $^{87}Sr/^{86}Sr$ ratios were previously published in González-Maurel et al. (2019a, 2019b) and are compiled in Supplementary Material Table SM1. The SiO_2 composition of the selected samples varies from 56.6 to 60.5% m/m, while $^{87}Sr/^{86}Sr$ ratios vary from 0.706176 to 0.706640 (Table 1).

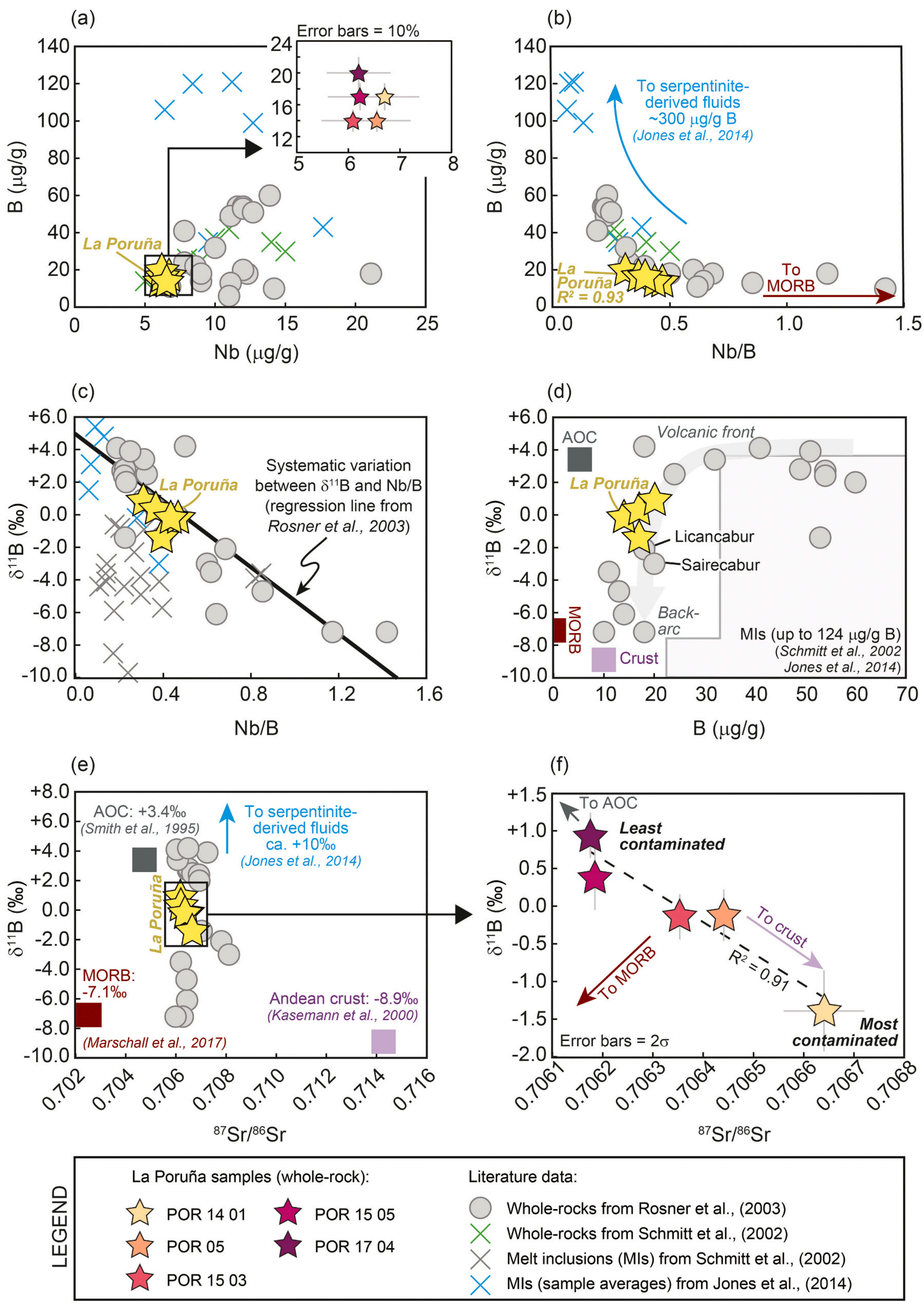

Fig. 4. Plots showing La Poruña whole-rock data from this study compared to Central Andean whole-rock and melt inclusion data from the literature. (a) B versus Nb, (b) B versus Nb/B, (c) $\delta^{11}B$ versus Nb/B, (d) $\delta^{11}B$ versus B, (e-f) $\delta^{11}B$ versus $^{87}Sr/^{86}Sr$. The new data for La Poruña overlap with the literature data for whole-rock lavas from the Central Andes. Note the strong co-variation between $\delta^{11}B$ and $^{87}Sr/^{86}Sr$ for La Poruña samples ($R^2 = 0.91$), where high $^{87}Sr/^{86}Sr$ is a proxy for crustal assimilation. Error bars are generally smaller than symbol size; in panel (f) error is 2σ. Literature data sources: Jones et al. (2014), Kasemann et al. (2000), Marschall et al. (2017), Rosner et al. (2003), Schmitt et al. (2002), Smith et al. (1995)

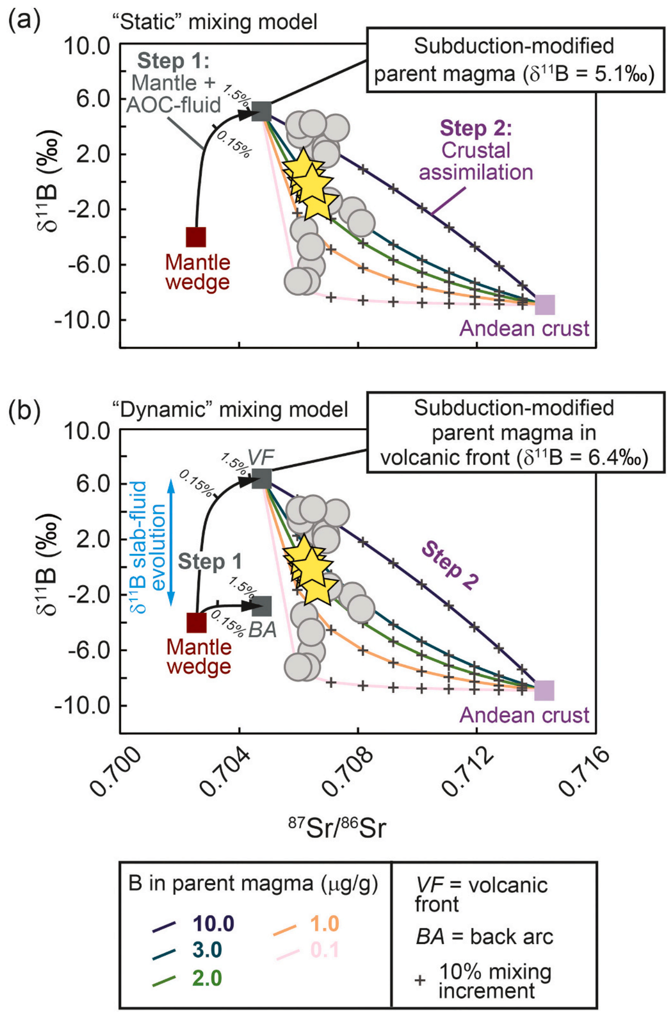

Fig. 5. Mixing models for B—Sr isotopes. These models are largely based on Rosner et al. (2003) and include "static" models (a), where no slab-fluid isotopic fractionation takes place and "dynamic" models (b), where the δ^{11}B value of the slab-derived fluid changes as a function of distance to the trench. The models involve two steps. In *Step 1*, a mantle-derived melt is mixed with < 2% of an AOC-derived slab fluid (Step 1 mixing curves shown after Rosner et al., 2003). This yields a subduction-modified parental arc melt with a δ^{11}B value of +5.1 ‰ in the static model and with δ^{11}B values between −2.8 ‰ (for addition of back arc fluids; BA) and + 6.4 ‰ (for addition of volcanic front fluids; VF) in the dynamic model. In *Step 2*, the subduction-modified parental melt is mixed with Andean continental crust. Note that in the dynamic model, a parental melt formed by mixing with relatively low δ^{11}B values (i.e. back arc) cannot reproduce the data from La Poruña. Therefore (and for clarity), *Step 2* mixing curves are not shown for a BA-modified parental melt in panel (b). Values for mantle wedge, AOC fluids, and Andean crust are from Table 3 in Rosner et al. (2003). Mixing curves are color-coded to the B content of the parent arc magma (0.1 to 10 μg/g). The La Poruña data can be explained by up to 20% mixing of continental crust into a subduction-modified, parental magma with relatively high initial δ^{11}B values (+5.1 to +6.4 ‰) and with B contents of around 2 to 3 μg/g.

3.2. Analysis of boron concentrations

Approximately 3 g of homogeneous sample powders were made into nano-particulate pressed pellets ("nano-pellets") following established methods (Garbe-Schönberg and Müller, 2014) at Kiel University using a FRITSCH Pulverisette 7 PL and slightly modified milling and tablet-pressing protocols. The nano-pellets were analyzed for multi-trace elemental abundances – including boron – at the ICPMS-Lab, Institute of Geosciences, Kiel University, Germany using an AGILENT 8900 ICP-MS/MS instrument coupled to a COHERENT 193 nm GeoLas HD laser ablation unit (for details see Garbe-Schönberg and Müller, 2014). Average analytical precision for all elements analyzed with five spots per pellet was 2.6% RSD (1SD) and 2.8% RSD for boron while average measurement uncertainty over the length of the session as determined from replicate measurements of the samples was 2.6% RSD for all trace elements but increased to 9.5% RSD for boron. Boron elemental data for all individual spot measurements on nano-pellets of the La Poruña samples and the reference materials are provided in Supplementary Material Table SM2.

3.3. Analysis of boron isotopes

The same nano-pellets on which elemental concentrations were determined in Kiel, were analyzed for δ^{11}B compositions at the MC-ICP-MS Facility, Department of Geological Sciences, University of Cape Town, South Africa using a Nu Instruments NuPlasma HR coupled to an ASI RESOlution SE 193 nm laser ablation unit. To maximize boron sensitivity, the NuPlasma HR was operated at 6 kV and fitted with a light-element, high-abundance skimmer cone. A laser spot size of 220 μm was used and scanned at 6 μm.*sec*$^{-1}$ along a 450 μm line, after rapid pre-ablation cleaning with a 240 μm spot. Ablation was conducted under helium (400 ml.min^{-1}) and nitrogen (9 ml.min^{-1}), blended with argon prior to injection into the plasma. A laser energy setting of 1.2 kV was used, which yielded an energy density of ±4.3 J.cm^{-2}. All analyses of unknown samples were bracketed with analyses of a JB-2 nano-pellet for which a δ^{11}B value of 7.12 ± 0.20 ‰ was assigned, enabling the referencing of all unknown sample δ^{11}B data to a ^{11}B/^{10}B ratio value of 4.04362 ± 0.001 for NIST SRM951 (Liu et al., 2018). The final δ^{11}B value of each unknown sample is the average of 4 successive JB-2-bracketed analyses with the 2σ values based on the reproducibility of these analyses and the propagated uncertainty of the reference values used for JB-2 and NIST SRM951. Results for reference materials with published boron isotope compositions and prepared as nano-pellets are reported in Table 1.

4. Results

The analyzed samples have boron contents ranging from 14 to 20 μg/g and δ^{11}B values ranging from −1.39 ± 0.54 to +0.94 ± 0.30 ‰ (2σ uncertainty; see Table 1). The new data reported here are plotted in Fig. 4 along with literature data for Central Andean whole-rocks (Rosner et al., 2003; Schmitt et al., 2002) and melt inclusions (Jones et al., 2014; Schmitt et al., 2002). The La Poruña data overlap with available whole-rock data, and in some cases, they appear to "fill a gap" in the arc-wide dataset of Rosner et al. (2003) (e.g. Fig. 4b-e). The La Poruña samples cluster at relatively low Nb and low B contents compared to the regional data (Fig. 4a) and their boron content increases with decreasing Nb/B, similarly to the literature whole-rock data (Fig. 4b). Notably, the Nb/B ratio of La Poruña samples is significantly lower than MORB (see arrow in Fig. 4b), which is typical for arc sample suites and indicates involvement of boron-rich, slab-derived fluids in petrogenesis (e.g. Ishikawa and Tera, 1997).

With respect to δ^{11}B values, the La Poruña samples plot close to the δ^{11}B versus Nb/B regression line constructed for a suite of Central Andean whole-rock lava samples by Rosner et al. (2003) (Fig. 4c). However, looking at the La Poruña samples in isolation shows that there is a rather weak correlation between δ^{11}B and Nb/B ($R^2 = 0.24$; not shown). On at a plot of δ^{11}B versus B, the La Poruña samples again overlap with the regional trend and plot close to samples from the near-by volcanoes Licancabur and Sairecabur (Fig. 4d). Finally, on a plot of δ^{11}B versus ^{87}Sr/^{86}Sr, we can see that the La Poruña samples plot within the space defined by the three geochemical end-members of Altered Ocean Crust (AOC), Mid-Ocean Ridge Basalt (MORB), and Andean continental crust (Fig. 4e). On closer inspection, a strong positive correlation between δ^{11}B and ^{87}Sr/^{86}Sr is revealed ($R^2 = 0.91$; Fig. 4f). This relationship will

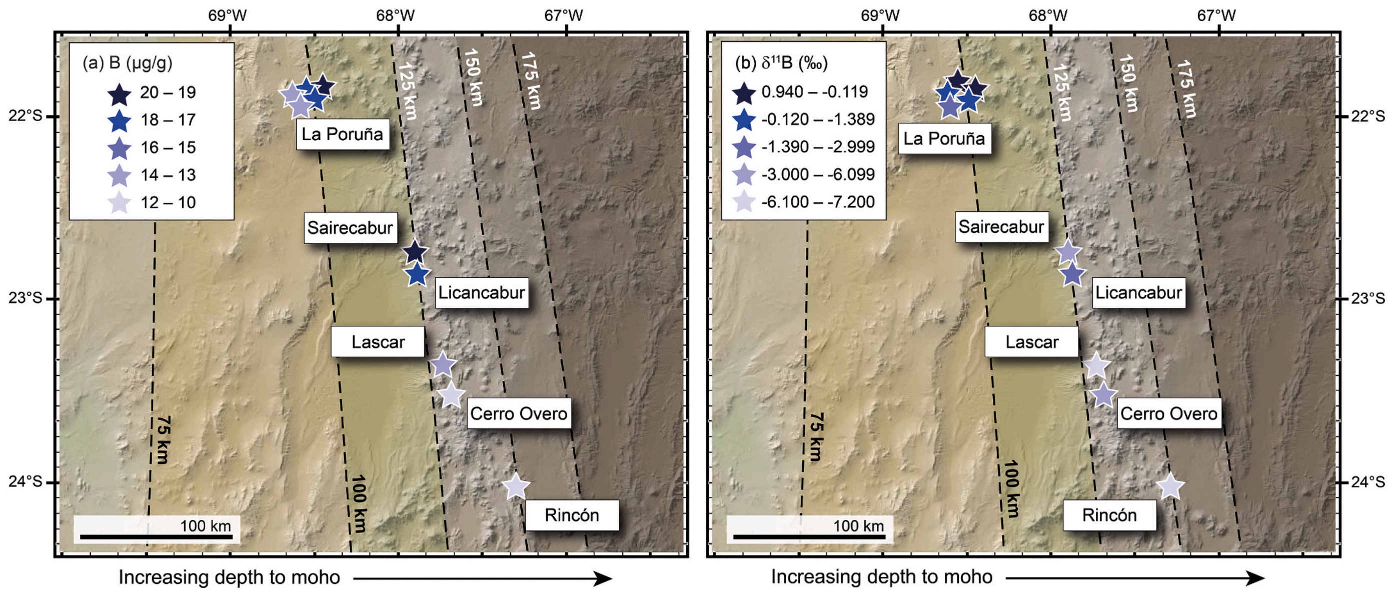

Fig. 6. Global Multi-Resolution Topography image for the Central Andes showing regional variations in (a) boron content (μg/g) and (b) δ^{11}B values (‰) in whole-rock lava samples from several volcanoes. Dashed lines represent the depth of the Wadatti-Benioff zones (after Cahill and Isacks, 1992). Data are from this study and Rosner et al. (2003). For analytical uncertainties see Methods. Background map made with GeoMapApp (www.geomapapp.org; Ryan et al., 2009).

be examined further in the Discussion section below.

5. Discussion

5.1. Overview of B contents and δ^{11}B values for La Poruña

Compared to the available whole-rock boron concentration data for the Central Andes, La Poruña has relatively low boron contents at 16 μg/g on average (Fig. 4a). There is a strong correlation between B and Nb/B among our samples ($R^2 = 0.93$; Fig. 4b). Since the Nb/B ratio is a proxy for fluid transfer in subduction zones, this relationship supports a role for slab-derived fluids at La Poruña, similar to what has been proposed for other arc lava suites (e.g. de Hoog and Savov, 2018; Ishikawa and Tera, 1997; Tonarini et al., 2001a). There is a weak positive correlation between B concentration and SiO_2 content ($R^2 = 0.48$; not shown). Although there is scatter in the data and the dataset is small, the overall increase in B with SiO_2 is consistent with B behaving as an incompatible element during differentiation (see also Schmitt et al., 2002).

Turning to the boron isotope data, La Poruña δ^{11}B values vary from −1.39 to +0.94 ‰ (Fig. 4, Table 1). These values agree well with boron isotope data from other volcanoes in the region (Fig. 4c-d) and they vary systematically with ^{87}Sr/^{86}Sr ratios obtained on the same samples (Fig. 4e-f). We will now explore potential reasons for these variations. As described above, boron isotope variations in volcanic arcs are often attributed to variable inputs of isotopically heterogeneous slab-derived fluids to the mantle wedge, which in turn may be related to the distance from the arc trench (e.g. Tonarini et al., 2001a; Rosner et al., 2003; Palmer, 2017; Agostini et al., 2021). Since La Poruña is a young, monogenetic volcanic complex, its distance from the arc front has remained fixed during its growth and evolution (González-Maurel et al., 2019b). Therefore, the observed variations in δ^{11}B values at La Poruña cannot be related to the geometry of the volcanic arc. The variations in δ^{11}B values at La Poruña may instead be a result of fractional crystallization. However, this hypothesis can be ruled out on the basis of the similar mineral content of the different lithofacies at La Poruña (González-Maurel et al., 2019b; Marín et al., 2020). Moreover, at La Poruña there is a change in δ^{11}B values of >2‰ over a relatively narrow SiO_2 range of ca. 4 % m/m, which is likely not due to fractional crystallization since boron isotopes are not expected to fractionate significantly during crystallization at high temperatures (see the fractionation models in Kaliwoda et al., 2011). There are also different δ^{11}B values among samples with similar volume % of vesicles, which leads us to rule out isotopic fractionation due to degassing (cf. Schmitt et al., 2002). In the section below, we will now consider crustal assimilation as a process that may have modified boron isotope ratios at La Poruña.

5.2. Crustal assimilation and mixing models

In Section 5.1 above we ruled out volcano-arc geometry, fractional crystallization, and degassing as factors controlling the variability in δ^{11}B values at La Poruña. Given that crustal assimilation is well documented both for the Central Andes at large and for La Poruña in particular (e.g. with respect to Sr and O isotopes; González-Maurel et al., 2019a, 2019b, González-Maurel et al., 2020), we now turn our focus to the question of whether the boron isotope variations at La Poruña reflect interaction between magma and its host rocks during crustal storage and ascent. Strontium isotopes are a good proxy for crustal contamination and co-vary significantly with δ^{11}B in our samples (Fig. 4f), whereby the most contaminated sample (i.e. the one with the highest ^{87}Sr/^{86}Sr ratio) has the lowest δ^{11}B value. This observation suggests that La Poruña parental magma assimilated a contaminant with high ^{87}Sr/^{86}Sr and low δ^{11}B values, such as the Andean continental crust (^{87}Sr/^{86}Sr = 0.71428, Ort et al., 1996 and δ^{11}B = −8.9 ‰, Kasemann et al., 2000). A similar scenario has previously been suggested for the Central Andes, as outlined below.

To explain regional variations in δ^{11}B values in the Central Andes, Rosner et al. (2003) suggested a two-step petrogenetic model. In the first step, primary mantle-like melts with relatively low δ^{11}B values and low ^{87}Sr/^{86}Sr ratios were mixed with ^{11}B-enriched AOC-derived slab fluids. In the models of Rosner et al. (2003), addition of small amounts (ca. 1.5%) of AOC-derived slab fluid to a mantle-derived melt yielded parental arc magmas with δ^{11}B values of ca. -2.8 to +6.4 ‰, depending on whether isotope fractionation across the arc was considered or not (i.e. from volcanic front to back arc). In the second stage of evolution, these subduction-modified parental arc melts were mixed with Andean continental crust, the latter of which is characterized by low δ^{11}B values of around −8.9 ‰ (Kasemann et al., 2000). These two stages of mixing were suggested by Rosner et al. (2003) as a way to explain the B contents and δ^{11}B values of their suite of Central Andean lavas. In Fig. 5 we present similar B—Sr isotope mixing models, but with additional mixing

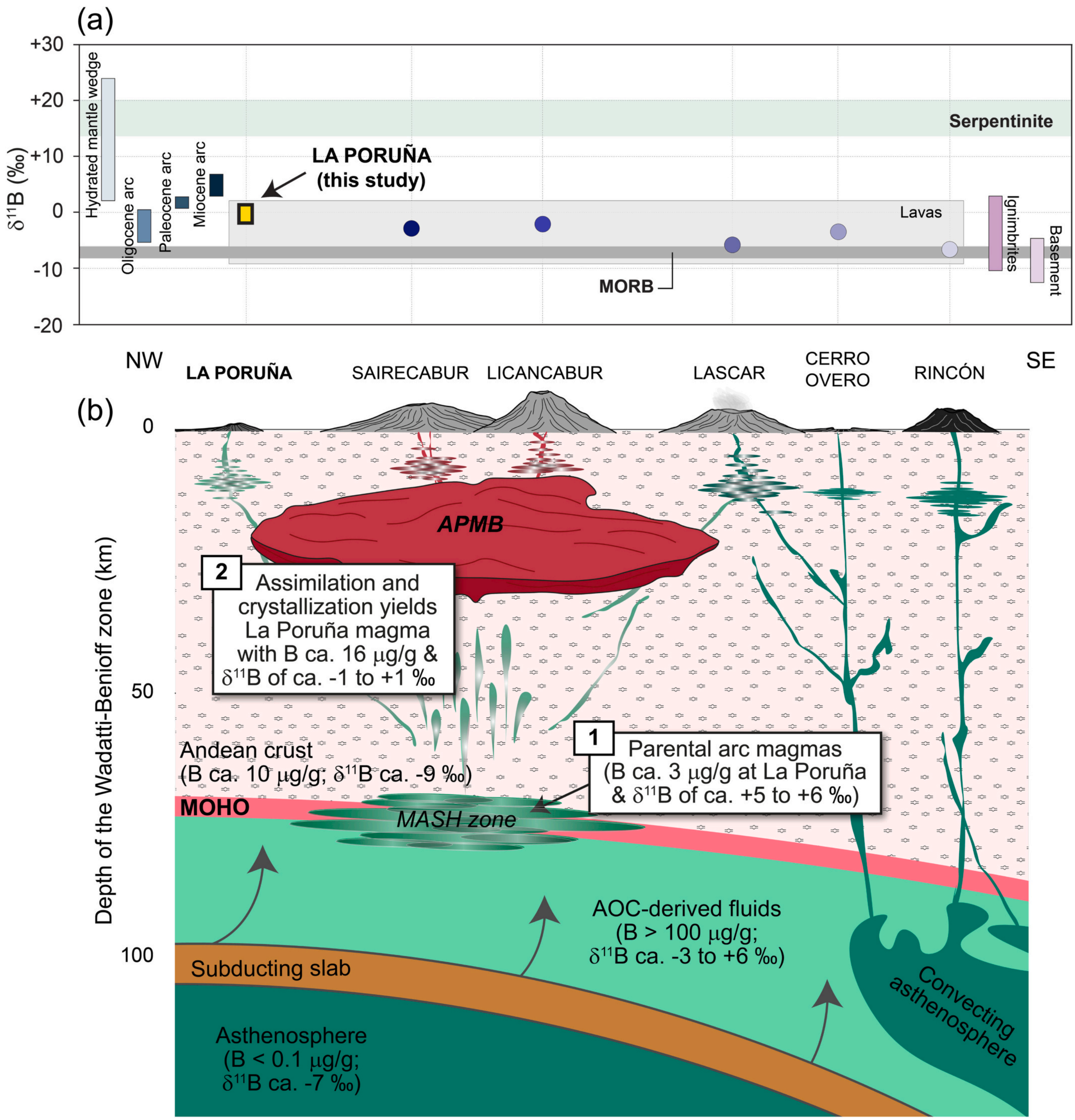

Fig. 7. a) Whole-rock δ^{11}B values of La Poruña (this work) compared to lavas (Rosner et al., 2003) and melt inclusions (averages from Jones et al., 2014) from the Central Andes. Also shown are the ranges of δ^{11}B values for Central Andean ignimbrites (Schmitt et al., 2002), Central Andean basement rocks (Kasemann et al., 2000), hydrated mantle wedge (Straub and Layne, 2002), MORB (Marschall et al., 2017), and serpentinite (Scambelluri and Tonarini, 2012). b) Schematic model for the Central Andes (between 21°-24°S) showing a variably subduction-modified sub-arc mantle and a thick continental crust wherein lies the Altiplano-Puna Magma Body (APMB). The B and B-isotope data for La Poruña (this study) suggest a subduction-modified parental arc magma with relatively high δ^{11}B values (+5.1 to +6.4 ‰) and with B contents of around 2 to 3 µg/g (see box 1). This parental magma then ascended through the arc crust where its δ^{11}B values were modified by crustal assimilation involving low δ^{11}B continental crust (see box 2). The magma plumbing system shown for La Poruña is based on Gonzalez-Maurel et al. (2019b).

curves that intersect the data for La Poruña. In order to satisfactorily explain the La Poruña data, we found that a subduction-modified parental arc magma with relatively high δ^{11}B values is required (i.e. around +5.1 to +6.4 ‰; see Fig. 5). We therefore suggest that at La Poruña the primary mantle source interacted with high δ^{11}B slab-derived fluids generated in the volcanic front and that there was little or no input of slab-derived fluids generated in the back arc, as these would have relatively low δ^{11}B values (see Rosner et al., 2003 and Fig. 5b). In summary, our models indicate that La Poruña magmas record up to 20% addition of Andean continental crust (δ^{11}B = −8.9 ‰) to a high δ^{11}B subduction-modified arc parental melt (δ^{11}B = +5.1 to +6.4‰) that contained ca. 3 µg/g boron. The amount of assimilation required to explain the data would vary depending on the exact end-members chosen (e.g. uncertainties exist around the exact nature of the slab-derived fluids involved and it may be an over-simplification to represent the Andean continental crust as a fixed point when it naturally has a range of values). Nonetheless, we offer broad constraints on the processes controlling $\delta^{11}B$ values at La Poruña that are consistent with the models presented in Rosner et al. (2003) and, notably, with the results of mixing models using oxygen isotopes where up to 28% crustal assimilation was suggested for this volcano (González-Maurel et al., 2020).

5.3. Regional perspective

Boron enrichment in volcanic arcs is generally thought to be due to addition of boron to the mantle melting region via slab-derived fluids (e.g. de Hoog and Savov, 2018; Ishikawa and Tera, 1997; Tonarini et al., 2001a). At La Poruña, an initially mantle-derived melt with very low B content (e.g. B = 0.07 μg/g for MORB; Marschall et al., 2017) was most likely modified by addition of small amounts of slab-derived fluids such that its boron content increased to around 2 to 3 μg/g, as indicated by our mixing models (Fig. 5). Subsequent crystallization would have led to an overall increase in B with SiO_2 as B is expected to behave as an incompatible element during differentiation (see also Schmitt et al., 2002).

Comparing our data for La Poruña (this study) to data for other Central Andean volcanoes (Rosner et al., 2003), we can see that lavas from Sairecabur and Licancabur volcanoes have lower $\delta^{11}B$ values than those of La Poruña, which we propose is due to higher degrees of assimilation of the low $\delta^{11}B$ Andean continental crust at those localities (Figs. 6 and 7). Indeed, greater degrees of crustal contamination towards the center of the Altiplano-Puna Magma Body have previously been suggested based on $^{87}Sr/^{86}Sr$ ratios and other geochemical characteristics of coeval volcanism within the Altiplano-Puna Volcanic Complex (e.g. Michelfelder et al., 2013; Godoy et al., 2017; González-Maurel et al., 2019a; Fig. 7). The broad-stroke differences in the B contents and $\delta^{11}B$ values of the group of volcanoes comprising La Poruña, Sairecabur, and Licancabur compared to the group comprising Lascar, Cerro Overo and Rincón (Fig. 6) imply variations whose underlying cause might be related to large-scale changes in subduction thermal conditions, slab fluid composition, and/or mantle composition (e.g. Comte et al., 2016; Contreras-Reyes et al., 2021; Gao et al., 2021; Godoy et al., 2019; Jones et al., 2014; Kay et al., 1994; Rosner et al., 2003). It is currently difficult to distinguish between these possibilities, especially when comparing data from low spatial resolution studies where only one or two data points per volcano are available. We stress here that detailed study of the boron isotopic variations at individual volcanic complexes in different parts of the Central Andes would be needed in order to clarify the sources of regional heterogeneities and to fully assess the relative roles of different subduction and crustal inputs along the arc.

6. Concluding remarks

The availability of geochemically well-characterized lava samples from La Poruña monogenetic scoria cone allowed for detailed investigation regarding how $\delta^{11}B$ values are modified as a consequence of crustal assimilation. La Poruña B contents range from 14 to 20 μg/g and $\delta^{11}B$ values range from -1.39 ± 0.54 ‰ (2σ) to $+0.94 \pm 0.30$ ‰ (2σ), which overlap with the range of available whole-rock data for Central Andean lavas. A striking feature of our data is that La Poruña $\delta^{11}B$ values correlate negatively with $^{87}Sr/^{86}Sr$ isotopic ratios obtained on the same samples ($R^2 = 0.91$). Since $^{87}Sr/^{86}Sr$ is a strong proxy for crustal contamination at La Poruña, the trend towards relatively low $\delta^{11}B$ values with increasing $^{87}Sr/^{86}Sr$ (i.e. with increasing degree of crustal contamination) suggests that the B isotope compositions of La Poruña magmas were controlled by assimilation of a crustal component with low $\delta^{11}B$ values and high $^{87}Sr/^{86}Sr$ ratios, such as the local Andean continental crust. Mixing models based on B and Sr isotopes support a broadly two-step magma evolution for La Poruña (summarized in Fig. 7). In step 1, mantle-derived primary melts interacted with boron-rich slab-derived fluids with high $\delta^{11}B$ values, which yielded subduction-modified parental magmas with ca. 3 μg/g B and relatively high $\delta^{11}B$ values. In step 2, the high $\delta^{11}B$ parental magmas ascended through the crust where they assimilated up to 20% crustal material, which further modified their $\delta^{11}B$ values and $^{87}Sr/^{86}Sr$ ratios. In comparison to available regional values for B and $\delta^{11}B$, it appears that La Poruña and nearby volcanic centers shared a similar source and magmatic history, while volcanoes south of 23°S differ. Deconvolving the roles of various subduction and crustal inputs in the Central Andes would require further studies on individual volcanoes along the arc.

Declaration of Competing Interest

Benigno Godoy reports financial support was provided by the National Fund For Scientific Technological and Technological Innovation Development and the National Commission for Scientific and Technological Research Funds for Research Centers in Priority Areas. Frances M. Deegan reports financial support was provided by the Swedish Research Council and Uppsala University. Petrus le Roux reports financial support was provided by the National Research Foundation of South Africa.

Acknowledgments

We thank Margaret Hartley for her thorough and thoughtful review that helped to improve this work. We also thank an anonymous reviewer for their input and Greg Shellnut for editorial handling. This work is based on research supported in part by funding from ANID "FONDECYT Iniciación Project" n°11200013 to B.G., the Swedish Research Council (*Vetenskapsrådet*) and the Section for Natural Resources and Sustainable Development (NRHU) at the Department of Earth Sciences, Uppsala University to F.M.D., and the National Research Foundation of South Africa (Grant number: 129318) to P.L.R.

Appendix A. Supplementary data

Supplementary data to this article can be found online at https://doi.org/10.1016/j.lithos.2023.107030.

References

Agostini, S., Di Giuseppe, P., Manetti, P., Doglioni, C., Conticelli, S., 2021. A heterogeneous subcontinental mantle under the African–Arabian Plate boundary revealed by boron and radiogenic isotopes. Sci. Rep. 11 (1), 1–13. https://doi.org/10.1038/s41598-021-90275-7.

Beck, S.L., Zandt, G., Myers, S.C., Wallace, T.C., Silver, P.G., Drake, L., 1996. Crustal thickness variations in the central Andes. Geology 24 (5), 407–410. https://doi.org/10.1130/0091-7613.

Cahill, T., Isacks, B.L., 1992. Seismicity and shape of the subducted Nazca plate. Journal of Geophysical Research: Solid Earth 97 (B12), 17503–17529. https://doi.org/10.1029/92JB00493.

Chmielowski, J., Zandt, G., Haberland, C., 1999. The Central Andean Altiplano-Puna magma body. Geophys. Res. Lett. 26 (6), 783–786. https://doi.org/10.1029/1999GL900078.

Comte, D., Carrizo, D., Roecker, S., Ortega-Culaciati, F., Peyrat, S., 2016. Three-dimensional elastic wave speeds in the northern Chile subduction zone: variations in hydration in the supraslab mantle. Geophysical Supplements to the Monthly Notices of the Royal Astronomical Society 207 (2), 1080–1105. https://doi.org/10.1093/gji/ggw318.

Contreras-Reyes, E., Díaz, D., Bello-González, J.P., Slezak, K., Potin, B., Comte, D., Maksymowicz, A., Ruiz, J.A., Osses, A., Ruiz, S., 2021. Subduction zone fluids and arc magmas conducted by lithospheric deformed regions beneath the central Andes. Sci. Rep. 11 (1), 1–12. https://doi.org/10.1038/s41598-021-02430-9.

de Hoog, J.C.M., Savov, I.P., 2018. Boron isotopes as a tracer of subduction zone processes. In: Marschall, H., Foster, G. (Eds.), Boron Isotopes: Advances in Isotope Geochemistry. Springer, Cham, pp. 217–247. https://doi.org/10.1007/978-3-319-64666-4_9.

de Silva, S.L., 1989. Altiplano-Puna volcanic complex of the central Andes. Geology 17 (12), 1102–1106. https://doi.org/10.1130/0091-7613.

de Silva, S.L., Kay, S.M., 2018. Turning up the heat: high-flux magmatism in the Central Andes. Elements 14, 245–250. https://doi.org/10.2138/gselements.14.4.245.

Deegan, F.M., Troll, V.R., Whitehouse, M.J., Jolis, E.M., Freda, C., 2016. Boron isotope fractionation in magma via crustal carbonate dissolution. Sci. Rep. 6 (1), 1–7. https://doi.org/10.1038/srep30774.

Feeley, T.C., Davidson, J.P., 1994. Petrology of calc-alkaline lavas at Volcán Ollagüe and the origin of compositional diversity at Central Andean stratovolcanoes. J. Petrol. 35 (5), 1295–1340. https://doi.org/10.1093/petrology/35.5.1295.

Gangjian, W., Jingxian, W., Ying, L., Ting, K., Zhongyuan, R., Jinlong, M., Yigang, X., 2013. Measurement on high-precision boron isotope of silicate materials by a single column purification method and MC-ICP-MS. J. Anal. At. Spectrom. 33, 606–612. https://doi.org/10.1039/c3ja30333k.

Gao, Y., Tilmann, F., van Herwaarden, D.P., Thrastarson, S., Fichtner, A., Heit, B., Yuan, X., Schurr, B., 2021. Full waveform inversion beneath the central Andes: Insight into the dehydration of the Nazca slab and delamination of the back-arc lithosphere. Journal of Geophysical Research: Solid Earth 126 (7). https://doi.org/10.1029/2021JB021984 e2021JB021984.

Garbe-Schönberg, D., Müller, S., 2014. Nano-particulate pressed powder tablets for LA-ICP-MS. J. Anal. At. Spectrom. 29 (6), 990–1000. https://doi.org/10.1039/C4JA00007B.

Gméling, K., Németh, K., Martin, U., Eby, N., Varga, Z., 2007. Boron concentrations of volcanic fields in different geotectonic settings. J. Volcanol. Geotherm. Res. 159 (1–3), 70–84. https://doi.org/10.1016/j.jvolgeores.2006.06.009.

Godoy, B., Wörner, G., Kojima, S., Aguilera, F., Simon, K., Hartmann, G., 2014. Low pressure evolution of arc magmas in thickened crust: the San Pedro-Linzor volcanic chain, Central Andes, Northern Chile. J. S. Am. Earth Sci. 52, 24–42. https://doi.org/10.1016/j.jsames.2014.02.004.

Godoy, B., Wörner, G., Le Roux, P., de Silva, S., Parada, M.A., Kojima, S., González-Maurel, O., Morata, D., Polanco, E., Martínez, P., 2017. Sr- and Nd- isotope variations along the pleistocene san Pedro – Linzor volcanic chain, N. Chile: tracking the influence of the upper crustal Altiplano-Puna magma body. J. Volcanol. Geotherm. Res. 341, 172–186. https://doi.org/10.1016/j.jvolgeores.2017.05.030.

Godoy, B., Taussi, M., González-Maurel, O., Renzulli, A., Hernández-Prat, L., le Roux, P., Morata, D., Menzies, A., 2019. Linking the mafic volcanism with the magmatic stages during the last 1 Ma in the main volcanic arc of the Altiplano-Puna Volcanic Complex (Central Andes). J. S. Am. Earth Sci. 95, 102295 https://doi.org/10.1016/j.jsames. 2019.102295.

Godoy, B., McGee, L., González-Maurel, O., Rodríguez, I., le Roux, P., Morata, D., Menzies, A., 2020. Upper crustal differentiation processes and their role in 238U-230Th disequilibria at the San Pedro-Linzor volcanic chain (Central Andes). J. S. Am. Earth Sci. 102, 102672 https://doi.org/10.1016/j.jsames.2020.102672.

González-Maurel, O., le Roux, P., Godoy, B., Troll, V.R., Deegan, F.M., Menzies, A., 2019a. The great escape: petrogenesis of low-silica volcanism of Pliocene to Quaternary age associated with the Altiplano-Puna Volcanic Complex of northern Chile (21°10′-22°50′S). Lithos 346–347, 105162. https://doi.org/10.1016/j.lithos.2019.105162.

González-Maurel, O., Godoy, B., le Roux, P., Rodríguez, I., Marin, C., Menzies, A., Bertin, D., Morata, D., Vargas, M., 2019b. Magmatic differentiation at La Poruña scoria cone, Central Andes, northern Chile: evidence for assimilation during turbulent ascent processes, and genetic links with mafic eruptions at adjacent San Pedro volcano. Lithos 338–339, 128–140. https://doi.org/10.1016/j.lithos.2019.03.033.

González-Maurel, O., Deegan, F.M., le Roux, P., Harris, C., Troll, V.R., Godoy, B., 2020. Constraining the sub-arc, parental magma composition for the giant Altiplano-Puna Volcanic Complex, northern Chile. Sci. Rep. 10, 6864. https://doi.org/10.1038/s41598-020-63454-1.

Hervig, R.L., Moore, G.M., Williams, L.B., Peacock, S.M., Holloway, J.R., Roggensack, K., 2002. Isotopic and elemental partitioning of boron between hydrous fluid and silicate melt. Am. Mineral. 87 (5–6), 769–774. https://doi.org/10.2138/am-2002-5-620.

Huppert, H.E., Sparks, R.S.J., 1985. Cooling and contamination of mafic and ultramafic magmas during ascent through continental crust. Earth Planet. Sci. Lett. 74 (4), 371–386. https://doi.org/10.1016/S0012-821X(85)80009-1.

Ishikawa, T., Tera, F., 1997. Source, composition and distribution of the fluid in the Kurile mantle wedge: constraints from across-arc variations of B/Nb and B isotopes. Earth Planet. Sci. Lett. 152 (1–4), 123–138. https://doi.org/10.1016/S0012-821X(97)00144-1.

Jones, R.E., de Hoog, J.C., Kirstein, L.A., Kasemann, S.A., Hinton, R., Elliott, T., Litvak, V. D., 2014. Temporal variations in the influence of the subducting slab on Central Andean arc magmas: evidence from boron isotope systematics. Earth Planet. Sci. Lett. 408, 390–401. https://doi.org/10.1016/j.epsl.2014.10.004.

Kaliwoda, M., Marschall, H.R., Marks, M.A., Ludwig, T., Altherr, R., Markl, G., 2011. Boron and boron isotope systematics in the peralkaline Ilímaussaq intrusion (South Greenland) and its granitic country rocks: a record of magmatic and hydrothermal processes. Lithos 125 (1–2), 51–64. https://doi.org/10.1016/j.lithos.2011.01.006.

Kasemann, S., Erzinger, J., Franz, G., 2000. Boron recycling in the continental crust of the Central Andes from the Paleozoic to Mesozoic, NW Argentina. Contrib. Mineral. Petrol. 140 (3), 328–343. https://doi.org/10.1007/s004100000189.

Kay, S.M., Coira, B., Viramonte, J., 1994. Young mafic back arc volcanic rocks as indicators of continental lithospheric delamination beneath the argentine Puna plateau, central Andes. Journal of Geophysical Research: Solid Earth 99 (B12), 24323–24339. https://doi.org/10.1029/94JB00896.

Konrad-Schmolke, M., Halama, R., 2014. Combined thermodynamic–geochemical modeling in metamorphic geology: boron as tracer of fluid–rock interaction. Lithos 208, 393–414. https://doi.org/10.1016/j.lithos.2014.09.021.

Liu, Y.-H., Huang, K.-F., Lee, D.-C., 2018. Precise and accurate boron and lithium isotopic determinations for small sample-size geological materials by MC-ICP-MS. J. Anal. At. Spectrom. 33, 846–855. https://doi.org/10.1039/c7ja00400a.

Mamani, M., Wörner, G., Sempere, T., 2010. Geochemical variations in igneous rocks of the Central Andean orocline (13°S to 18°S): tracking crustal thickening and magma generation through time and space. Geol. Soc. Am. Bull. 122 (1–2), 162–182. https://doi.org/10.1130/B26538.1.

Marín, C., Rodríguez, I., Godoy, B., González-Maurel, O., Le Roux, P., Medina, E., Bertín, D., 2020. Eruptive history of La Poruña scoria cone, Central Andes, Northern Chile. Bulletin of Volcanology 82 (11), 1–19. https://doi.org/10.1007/s00445-020-01410-7.

Marschall, H.R., Altherr, R., Rüpke, L., 2007. Squeezing out the slab—modelling the release of Li, be and B during progressive high-pressure metamorphism. Chem. Geol. 239 (3–4), 323–335. https://doi.org/10.1016/j.chemgeo.2006.08.008.

Marschall, H.R., Wanless, D., Shimizu, N., Pogge von Strandmann, P.A.E., Elliott, T., Monteleone, B.D., 2017. The boron and lithium isotopic composition of mid-ocean ridge basalts and the mantle. Geochim. Cosmochim. Acta 207, 102–138. https://doi.org/10.1016/j.gca.2017.03.028.

Matteini, M., Mazzuoli, R., Omarini, R., Cas, R., Maas, R., 2002. Geodynamical evolution of Central Andes at 24°S as inferred by magma composition along the Calama–Olacapato–El Toro transversal volcanic belt. J. Volcanol. Geotherm. Res. 118 (1–2), 205–228. https://doi.org/10.1016/S0377-0273(02)00257-3.

Michelfelder, G.S., Feeley, T.C., Wilder, A.D., Klemetti, E.W., 2013. Modification of the continental crust by subduction zone magmatism and vice-versa: Across-strike geochemical variations of silicic lavas from individual eruptive centers in the Andean Central volcanic zone. Geosciences 3 (4), 633–667. https://doi.org/10.3390/geosciences3040633.

Ort, M.H., Coira, B.L., Mazzoni, M.M., 1996. Generation of a crust-mantle mixture: Magma sources and contamination at Cerro Panizos, Central Andes. Contrib. Mineral. Petrol. 123, 308–322. https://doi.org/10.1007/s004100050158.

Palmer, M.R., 2017. Boron cycling in subduction zones. Elements: An International Magazine of Mineralogy, Geochemistry, and Petrology 13 (4), 237–242. https://doi.org/10.2138/gselements.13.4.237.

Palmer, M.R., Swihart, G.H., 1996. Boron isotope geochemistry: an overview. In: Grew, E.S., Anovitz, L.M. (Eds.), Boron: Mineralogy, Petrology and Geochemistry. Rev. Mineral. Geochem. 33, 709–744. https://doi.org/10.1515/9781501509223-015.

Peacock, S.M., Hervig, R.L., 1999. Boron isotopic composition of subduction-zone metamorphic rocks. Chem. Geol. 160 (4), 281–290. https://doi.org/10.1016/S0009-2541(99)00103-5.

Prezzi, C.B., Götze, H-J., Schmidt, S., 2009. 3D denisty model of the Central Andes. Phys. Earth Planet. Inter. 177, 217–234. https://doi.org/10.1016/j.pepi.2009.09.004.

Rosner, M., Erzinger, J., Franz, G., Trumbull, R.B., 2003. Slab-derived boron isotope signatures in arc volcanic rocks from the Central Andes and evidence for boron isotope fractionation during progressive slab dehydration. Geochem. Geophys. Geosyst. 4 (8) https://doi.org/10.1029/2002GC000438.

Ryan, J.G., Chauvel, C., 2014. The subduction-zone filter and the impact of recycled materials on the evolution of the mantle. In: Holland, H.D., Turekian, K.K. (Eds.), Treatise on Geochemistry, Second edition. Elsevier, pp. 479–508. https://doi.org/10.1016/B978-0-08-095975-7.00211–4.

Ryan, W.B.F., Carbotte, S.M., Coplan, J., O'Hara, S., Melkonian, A., Arko, R., Weissel, R. A., Ferrini, V., Goodwillie, A., Nitsche, F., Bonczkowski, J., Zemsky, R., 2009. Global Multi-Resolution Topography (GMRT) synthesis data set. Geochem. Geophys. Geosyst. 10 (3), Q03014. https://doi.org/10.1029/2008GC002332.

Scambelluri, M., Tonarini, S., 2012. Boron isotope evidence for shallow fluid transfer across subduction zones by serpentinized mantle. Geology 40 (10), 907–910. https://doi.org/10.1130/G33233.1.

Schmitt, A.K., Kasemann, S., Meixner, A., Rhede, D., 2002. Boron in central Andean ignimbrites: implications for crustal boron cycles in an active continental margin. Chem. Geol. 183 (1–4), 333–347. https://doi.org/10.1016/S0009-2541(01)00382-5.

Smith, H.J., Spivack, A.J., Staudigel, H., Hart, S.R., 1995. The boron isotopic composition of altered oceanic crust. Chem. Geol. 126, 119–135. https://doi.org/10.1016/0009-2541(95)00113-6.

Spandler, C., Pirard, C., 2013. Element recycling from subducting slabs to arc crust: a review. Lithos 170, 208–223. https://doi.org/10.1016/j.lithos.2013.02.016.

Spang, A., Baumann, T.S., Kaus, B.J., 2021. A Multiphysics Approach to Constrain the Dynamics of the Altiplano-Puna Magmatic System. Journal of Geophysical Research: Solid. Earth 126 (7). https://doi.org/10.1029/2021JB021725 e2021JB021725.

Straub, S.M., Layne, G.D., 2002. The systematics of boron isotopes in Izu arc front volcanic rocks. Earth Planet. Sci. Lett. 198 (1–2), 25–39. https://doi.org/10.1016/S0012-821X(02)00517-4.

Tonarini, S., Leeman, W.P., Ferrara, G., 2001a. Boron isotopic variations in lavas of the Aeolian volcanic arc, South Italy. J. Volcanol. Geotherm. Res. 110 (1–2), 155–170. https://doi.org/10.1016/S0377-0273(01)00203-7.

Tonarini, S., Armienti, P., D'Orazio, M., Innocenti, F., 2001b. Subduction-like fluids in the genesis of Mt. Etna magmas: evidence from boron isotopes and fluid mobile elements. Earth Planet. Sci. Lett. 192 (4), 471–483. https://doi.org/10.1016/S0012-821X(01)00487-3.

Trumbull, R., Riller, U., Oncken, O., Scheuber, E., Munier, K., Hongn, F., 2006. The time-space distribution of Cenozoic volcanism in the South-Central Andes: A new data compilation and some tectonic implications. In: Oncken, O., Chong, G., Franz, G., Giese, P., Götze, H.-J., Ramos, V.A., Strecker, M.R., Wigger, P. (Eds.), The Andes: Active Subduction Orogeny, pp. 29–43. https://doi.org/10.1007/978-3-540-48684-8_2.

van Alderwerelt, B., Ukstins, I.A., Ramos, F.C., 2021. Sr isotopes and geochemistry of Cerro Overo maar provide a unique window into arc magma genesis in the Central

Volcanic Zone of the Andes. Lithos 386, 105978. https://doi.org/10.1016/j.lithos.2021.105978.

Ward, K.M., Zandt, G., Beck, S.L., Christensen, D.H., McFarlin, H., 2014. Seismic imaging of the magmatic underpinnings beneath the Altiplano-Puna volcanic complex from the joint inversion of surface wave dispersion and receiver functions. Earth Planet. Sci. Lett. 404, 43–53. https://doi.org/10.1016/j.epsl.2014.07.022.

Wörner, G., Hammerschmidt, K., Henjes-Kunst, F., Lezaun, J., Wilke, H., 2000. Geochronology (40Ar/39Ar, K-Ar and He-exposure ages) of Cenozoic magmatic rocks from northern Chile (18 22°S): implications for magmatism and tectonic evolution of the central Andes. Revista Geológica de Chile 27 (2), 205–240. https://doi.org/10.4067/S0716-02082000000200004.

Wörner, G., Mamani, M., Blum-Oeste, M., 2018. Magmatism in the Central Andes. Elements 14, 237–244. https://doi.org/10.2138/gselements.14.4.237.

Zandt, G., Leidig, M., Chmielowski, J., Baumont, D., Yuan, X., 2003. Seismic detection and characterization of the Altiplano-Puna magma body, central Andes. Pure Appl. Geophys. 160 (3–4), 789–807. https://doi.org/10.1007/PL00012557.